Jass 2006
St. Petersburg

Daniela Gewald

Dynamics and Control of Hexapod Systems

1. Summary

A strategy for the combined tracking and vibration control of a parallel mechanism is presented. The investigated mechanism is a hexapod system with six degrees-of-freedom (DOF) that can realize accurate motions of the tool center point (TCP). To compensate mechanical vibrations transfered from the environment to the TCP, an active stabilization scheme based on a feedforward-feedback controller is applied. The feedforward controller should compensate most of the vibration forces and decouples the nonlinear hexapod dynamics, whereas the feedback controller compensates residual TCP-vibrations and provides the desired tracking task. Some simulations have been carried out, prooving the high performance of the combined stabilization and tracking system.

2. Introduction

Many devices that are sensible to mechanical vibrations require a system that decouple this devices from the vibrating environment. The vibration isolation system that is investigated in this paper is a parallel kinematic with six DOF, often referred to as hexapod or Gough-Stewart-platform ([1], [2]). The hexapod consists of a lower and an upper platform, that are linked by joints with six legs which are variable in length. On the one hand, the TCP can be aligned in all six DOF and on the other hand the upper platform can be isolated from ground vibrations which affect the lower platform (Fig. 1).

Figure 1: Hexapod system for tracking purposes (left) and stabilization of the upper platform (right)

Thus, a device that is mounted on the upper platform can be isolated from ground vibrations *and* can execute a required tracking or positioning task at the same time. Applications where both these features are needed are mobile tracking systems, like a telescope or an antenna on an aircraft or on a ship [3].

Examples of the use of Hexapod systems

Motion generator for flight simulators

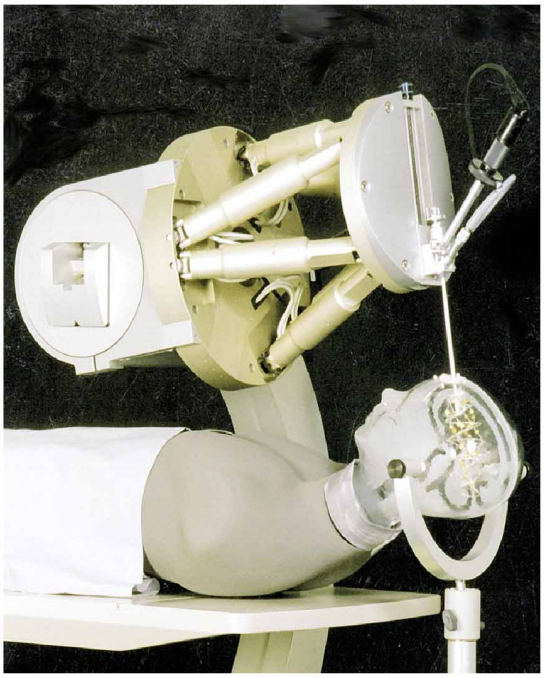

Applications in medical technology

Antenna precision alignment;
motion control for telescopes

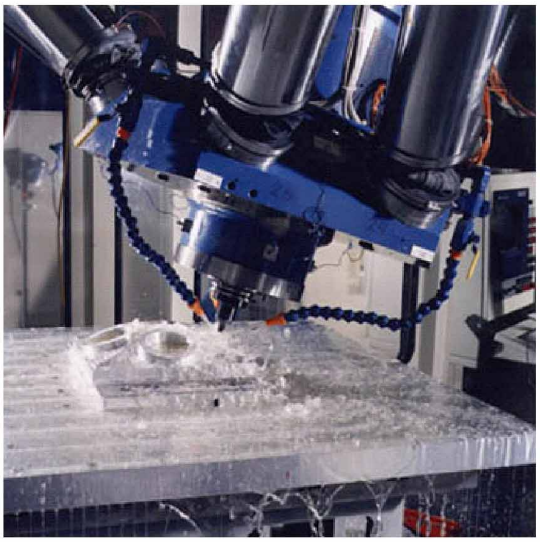

Applications in machine tools for highly precise motion between tool and work piece

This contribution is focused mainly on the control and simulation to prove the feasibility of the coupled stabilization/tracking system. The aim is to compensate vibration amplitudes up to 80 mm in a frequency range up to 5 Hz while the TCP is in tracking motion. The test rig to test and to verify the achieved results is still under construction. It consists of six electromechanical axes that are designed with ball screw assemblies which are driven by brushless AC-motors (Fig. 3).

3 Kinematics

The kinematics of Stewart-Gough platforms is a broad field of research and an essential requirement to provide a desired TCP motion. The solution of the geometrical relation between the TCP position resp. orientation and the six leg lengths can be obtained either by applying an inverse calculation scheme (inverse kinematics) or by using a forward kinematics algorithm (direct kinematics). In figure 3, the basic geometry of one leg with the moveable frame {**M**} and the fixed base frame {**I**} is shown, that will be used to derive the geometrical relations. The inverse kinematics describes the relation between a

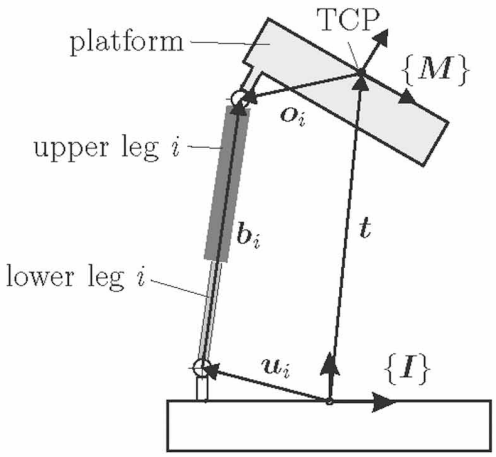

Figure 3: Topology of a Stewart-Gough platform (one leg)

given TCP-vector and the resulting lengths of the six legs. This algebraic relationship is described by six nonlinear equations that can be solved unique by

$$ {}_I\boldsymbol{b}_i = {}_I\boldsymbol{t} + \boldsymbol{T}_{IM} \cdot {}_M\boldsymbol{o}_i - {}_I\boldsymbol{u}_i, \tag{1} $$

$$ b_i = \sqrt{{}_I\boldsymbol{b}_i^T \cdot {}_I\boldsymbol{b}_i}, \tag{2} $$

with the leg lengths b_i $(i = 1...6)$ resulting from a desired TCP-alignment

$$ \boldsymbol{q} = \begin{pmatrix} {}_I\boldsymbol{t} & \boldsymbol{\phi} \end{pmatrix}^T = \begin{pmatrix} x_p & y_p & z_p & \alpha_p & \beta_p & \gamma_p \end{pmatrix}^T. \tag{3} $$

The rotation matrix $\boldsymbol{T}_{IM}$ is a function of the rotation angles α_p, β_p and γ_p of the TCP and is defined by three cardan rotations (x-y-z-series).

The direct kinematics computes the TCP position ${}_I\boldsymbol{t}$ and the TCP orientation $\boldsymbol{\phi}$ when a set of six leg lengths b_i is given. Generally, this quite complex analytical problem results in ambiguous solutions because the developed algorithms are based on polynomials of very high order. For example, Husty [19] and Innocenti [20] proposed different algorithms that compute 40th order polynomials and thus result in a relative high number of possible TCP-locations for a given set of leg lengths. Unfortunately, these analytical solutions are very CPU-intensiv; a basic problem in real-time control systems. A yet faster scheme to solve the direct kinematics is provided by the Newton-approach, a numerical scheme that is based on successive approximation. To make sure that the correct local solution is found, the Newton-approach has to be initialized with consistent initial TCP-conditions. The calculation scheme is then given by

$$ \boldsymbol{q}_{ap,k+1} = \boldsymbol{q}_{ap,k} + \boldsymbol{J}_p^{-1}(\boldsymbol{q}_{ap,k}) \cdot (\boldsymbol{b} - \boldsymbol{H}\left(\boldsymbol{q}_{ap,k}\right)), \tag{4} $$

The probably most important matrix for Stewart-Gough mechanisms is the platform Jacobian, describing the relation between the norm of the leg velocities $\dot{b}_i$ ($i = 1..6$) (resp. the gimbal point velocities) and the TCP-velocities $\dot{\boldsymbol{q}}$. With the unit vector

$$ {}_I\boldsymbol{e}_{b,i} = \frac{{}_I\boldsymbol{b}_i}{b_i}, \tag{16} $$

the norm of the velocity of leg i is

$$ \begin{aligned} \dot{b}_i =& {}_I\boldsymbol{e}_{b,i}^T \cdot \dot{\boldsymbol{t}} + {}_I\boldsymbol{e}_{b,i}^T \cdot (\boldsymbol{\omega} \times (\boldsymbol{T}_{IM} \cdot {}_M\boldsymbol{o}_i)) \\ =& \frac{1}{b_i} \cdot \left({}_I\boldsymbol{b}_i^T \cdot \dot{\boldsymbol{t}} + {}_I\boldsymbol{b}_i^T \cdot (\boldsymbol{\omega} \times (\boldsymbol{T}_{IM} \cdot {}_M\boldsymbol{o}_i)) \right). \end{aligned} \tag{17} $$

Here, the translation velocity of the upper platform is $\dot{\boldsymbol{t}}$ and the rotation velocity of the upper platform is $\boldsymbol{\omega}$. To simplify the calculation scheme, the skew symmetric "tilde"-tensor is used [14]:

$$ \boldsymbol{a} \times \boldsymbol{b} = \tilde{\boldsymbol{a}} \cdot \boldsymbol{b} = \tilde{\boldsymbol{b}}^T \cdot \boldsymbol{a} \tag{18} $$

After substituting the inverse kinematics equations (1) and (2) in eq. (17), using the tilde tensor and some additional transformations, a relation for the norm of the articular velocities with separated generalized velocities follows.

$$ \dot{b}_i = \frac{1}{b_i} \cdot \left\{ \left[{}_I\tilde{\boldsymbol{o}}_i \cdot ({}_I\boldsymbol{t} - {}_I\boldsymbol{u}_i) \right]^T \cdot \boldsymbol{\omega} + ({}_I\boldsymbol{t} - {}_I\boldsymbol{u}_i + {}_I\boldsymbol{o}_i)^T \cdot \dot{\boldsymbol{t}} \right\} \tag{19} $$

By applying this procedure to all six legs and allocating the elements in a matrix,

$$ \begin{aligned} \begin{pmatrix} \dot{b}_1 \\ \vdots \\ \dot{b}_6 \end{pmatrix} &= \begin{pmatrix} \frac{1}{b_1} \cdot ({}_I\boldsymbol{t} - {}_I\boldsymbol{u}_1 + \boldsymbol{T}_{IM} \cdot {}_M\boldsymbol{o}_1)^T & \frac{1}{b_1} \cdot ({}_I\tilde{\boldsymbol{o}}_1 \cdot ({}_I\boldsymbol{t} - {}_I\boldsymbol{u}_1))^T \\ \vdots & \vdots \\ \frac{1}{b_6} \cdot ({}_I\boldsymbol{t} - {}_I\boldsymbol{u}_6 + \boldsymbol{T}_{IM} \cdot {}_M\boldsymbol{o}_6)^T & \frac{1}{b_6} \cdot ({}_I\tilde{\boldsymbol{o}}_6 \cdot ({}_I\boldsymbol{t} - {}_I\boldsymbol{u}_6))^T \end{pmatrix} \cdot \begin{pmatrix} \dot{\boldsymbol{t}} \\ \boldsymbol{\omega} \end{pmatrix} \\ &= \boldsymbol{J}_p \cdot \dot{\boldsymbol{q}}, \end{aligned} \tag{20} $$

the Jacobian $\boldsymbol{J}_p$ of the platform is obtained, that was already introduced in eq. (4) to calculate the direct kinematics numerically. The platform Jacobi matrix can give important information about the geometrical condition of the system and is an important tool for singularity analysis [13], [12].

Generally, three different singularities may occur. The most simple singularity is based on the parameterisation of the rotation matrix $\boldsymbol{T}_{IM}$. If e.g. Euler-angles are chosen to describe the rotation sequences, then it may occur that at an angle of 90 degree a singularity appears. A second and more descriptive singularity occurs when the platform Jacobian is not regular, resulting in a structural singularity due to infinite leg forces. Thirdly, if the inverse Jacobian matrix happens to be singular, the Stewart-Gough mechanism loses a DOF.

To make sure that the mechanism is not moving to a singular configuration, the determinant of the Jacobi-matrix can be used as a measure for the actual platform configuration. The introduced mechanism in figure 1 has a singularity-free workspace, because the joint limits would be exceeded before a singular configuration is reached.

4 Dynamics

Generally, the Jacobians describe the relation
between the velocities of the independent coordinates $\dot{\boldsymbol{q}} = \begin{pmatrix} \dot{\boldsymbol{t}} & \boldsymbol{\omega} \end{pmatrix}^T$ and the velocities $\dot{\boldsymbol{x}}_i$ resp. $\boldsymbol{\Omega}_i$ of the corresponding body, which leads to

$$\dot{\boldsymbol{x}}_i = \boldsymbol{J}_{T,i} \cdot \dot{\boldsymbol{q}}, \tag{21}$$

and

$$\boldsymbol{\Omega}_i = \boldsymbol{J}_{R,i} \cdot \dot{\boldsymbol{q}}. \tag{22}$$

Thus, the accelerations can be obtained by

$$\ddot{\boldsymbol{x}}_i = \boldsymbol{J}_{T,i} \cdot \ddot{\boldsymbol{q}} + \dot{\boldsymbol{J}}_{T,i} \cdot \dot{\boldsymbol{q}}, \tag{23}$$

and

$$\dot{\boldsymbol{\Omega}}_i = \boldsymbol{J}_{R,i} \cdot \ddot{\boldsymbol{q}} + \dot{\boldsymbol{J}}_{R,i} \cdot \dot{\boldsymbol{q}}. \tag{24}$$

Fortunately, the characteristic of parallel robots is that many identically designed components are used. This reduces the number of structurally different Jacobi matrices to four (platform, lower legs, upper legs and lower universal joints) that only differ in their parameterisation. The Jacobians are developed kinematically in terms of vector geometry. The procedure is always the same, i.e. considering the constraint equations by establishing and combining two kinematic relations that describe the motion of the corresponding body in a base frame.
However, if the complete state of each body is known, then the dynamics of the Stewart-Gough-Platform can be derived in closed form by means of the Newton-Euler matrix formulation [14]:

$$\sum_{i=1}^{n} \boldsymbol{J}_{T,i}^T \left(\dot{\boldsymbol{p}}_i^{cog} - \boldsymbol{F}_i^e \right) + \boldsymbol{J}_{R,i}^T \left(\dot{\boldsymbol{L}}_i^{0'} - \boldsymbol{M}_i^{e,0'} \right) = \boldsymbol{0}, \tag{25}$$

with the active forces $\boldsymbol{M}_i^e$ resp. $\boldsymbol{F}_i^e$, the change of linear momentum

$$\dot{\boldsymbol{p}}_i^{cog} = m_i \cdot \ddot{\boldsymbol{x}}_{cog,i}, \tag{26}$$

the change of angular momentum related to a reference frame $0'$

$$\dot{\boldsymbol{L}}_i^{0'} = \boldsymbol{\Theta}_i^{0'} \cdot \dot{\boldsymbol{\omega}}_i + \tilde{\boldsymbol{\omega}}_i \cdot \boldsymbol{\Theta}_i^{0'} \cdot \boldsymbol{\omega}_i, \tag{27}$$

and the mass m_i and the moment of inertia $\boldsymbol{\Theta}_i^{0'}$ of body i. By using this method, the equations of motion can be obtained as an ODE-formulation related to the fixed $\{\boldsymbol{I}\}$-frame.

Platform Dynamics

Figure 6 shows the platform as an unconstrained body with the mass m_p and the inertial tensor $\boldsymbol{\Theta}_p$. To provide a more variable formulation with respect to possible applications,

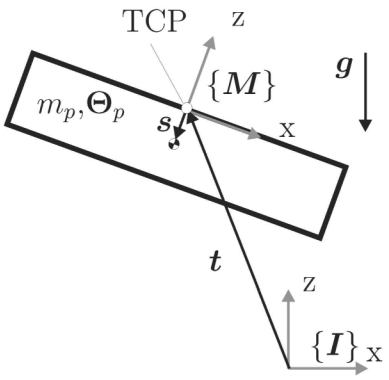

Figure 6: Platform as unconstrained body in space

the vector $\boldsymbol{s}$ can be changed by parameterisation with respect to the center of gravity of another body that is fixed on the upper platform and represents a load that could be e.g. a drilling tool or a telescope. The only active forces affecting the TCP are assumed as the gravity forces. The servo forces generating a desired TCP motion will be considered later. For this case, the derivation of the dynamic forces/moments of the platform is an easy task, because the independent TCP coordinates $\boldsymbol{q}$ are the platform DOF, given in the $\{\boldsymbol{I}\}$-frame.

$$\begin{pmatrix} \dot{\boldsymbol{p}} - \boldsymbol{F}_i^e \\ \dot{\boldsymbol{L}} - \boldsymbol{M}_i^e \end{pmatrix}_p = \begin{pmatrix} diag\{m_p\} & \boldsymbol{0} \\ m_p \cdot {}_I\tilde{\boldsymbol{s}} & {}_I\boldsymbol{\Theta}_p \end{pmatrix} \cdot \ddot{\boldsymbol{q}} + \begin{pmatrix} m_p \cdot \left(\dot{\tilde{\boldsymbol{\omega}}} + \tilde{\boldsymbol{\omega}} \cdot \tilde{\boldsymbol{\omega}}\right) \cdot {}_I\boldsymbol{s} \\ \tilde{\boldsymbol{\omega}} \cdot {}_I\,\boldsymbol{\Theta}_p \cdot \boldsymbol{\omega} \end{pmatrix} - m_p \cdot \begin{pmatrix} \boldsymbol{g} \\ {}_I\tilde{\boldsymbol{s}} \cdot \boldsymbol{g} \end{pmatrix} \tag{28}$$

Here, ${}_I\boldsymbol{s} = \boldsymbol{T}_{IM} \cdot {}_M\boldsymbol{s}$ is the COG-vector transformed to the $\{\boldsymbol{I}\}$-frame and ${}_I\boldsymbol{\Theta}_p = \boldsymbol{T}_{MI} \cdot \left({}_M\boldsymbol{\Theta}_p^{cog} - {}_M\tilde{\boldsymbol{s}} \cdot {}_M\tilde{\boldsymbol{s}}^T \cdot m_p\right) \cdot \boldsymbol{T}_{IM}$ is the transformed inertial tensor with respect to the frame displacement. In the Newton-Euler equations, the first three lines in the dynamic ratio describe the forces generated by the change of impulse and the last three lines are the result of a change in the angular momentum. If the platform-COG would be identical with the TCP ($\boldsymbol{s} = \boldsymbol{0}$), eq. (28) would describe the decoupled and well known principles of angular momentum and linear momentum [11].

5 Ideal Stabilization

In an ideal system, a perfect vibration isolation can be achieved with a feedforward control when the model of the system is known exactly. This can be seen if the problem is reduced to a simple rigid and friction-free one DOF system that is illustrated in Fig. 2 (left).

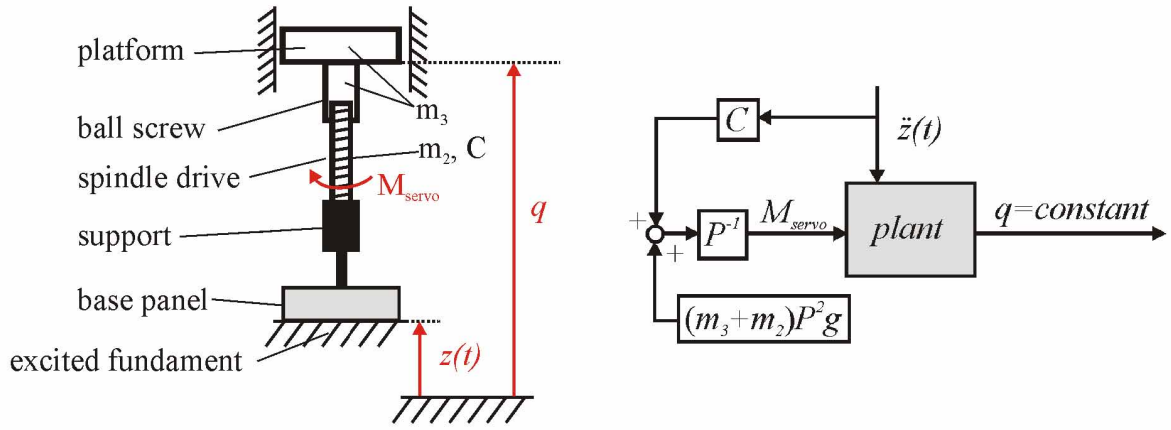

Figure 2: Topology of a 1-DOF vibration isolation system (left) and ideal feedforward vibration compensation (right)

The system consists of a base panel which is fixed to a spindle support, a spindle (mass m_2, rotational inertia C) and a platform that is mounted on a ball screw (mass m_3).
By applying a servo moment M_{servo} to the spindle, the rotation of the spindle is transfered in a translation of the ball screw and the upper platform can be moved in vertical direction.

When undesired vibrations *z(t)* affect the base panel now, they are transfered to the platform. To block the transmission of the vibrations and to keep *q* at a desired constant value, the servo moment has to hold the platform/ball screw statically and additionally it has to generate the angular acceleration of the spindle.
That means, perfect vibration isolation is achieved when the servo moment is

$$M_{servo} = \frac{1}{P}\left(C\,\ddot{z} + (m_2 + m_3)P^2\,g\right), \qquad (1)$$

where *P* is the pitch of the spindle. Fig. 2 (right) shows the corresponding feedforward control.
The same procedure can be applied to the hexapod system to block the transmission of six DOF vibrations. But here, the equations of motion are more complex, because we have to deal with a multi-input multi-output system (MIMO) due to the closed kinematical loops. But the same closed kinematical loops that couple the dynamics provide a favorably high stiffness what makes it possible to assume a rigid multi body system (MBS). The equations of motion are derived in minimal coordinates by means of the Newton-Euler approach. The system consists of 19 bodies: The six cylinders with the ball screws, the six spindle bodies, the six lower supports with the motors and the upper platform. Fig. 3 shows the hexapod topology with one leg (left) and the test rig that has been investigated (right). It should be noted that the photo on the right shows the first version of the hexapod that is right now in the redesign process.

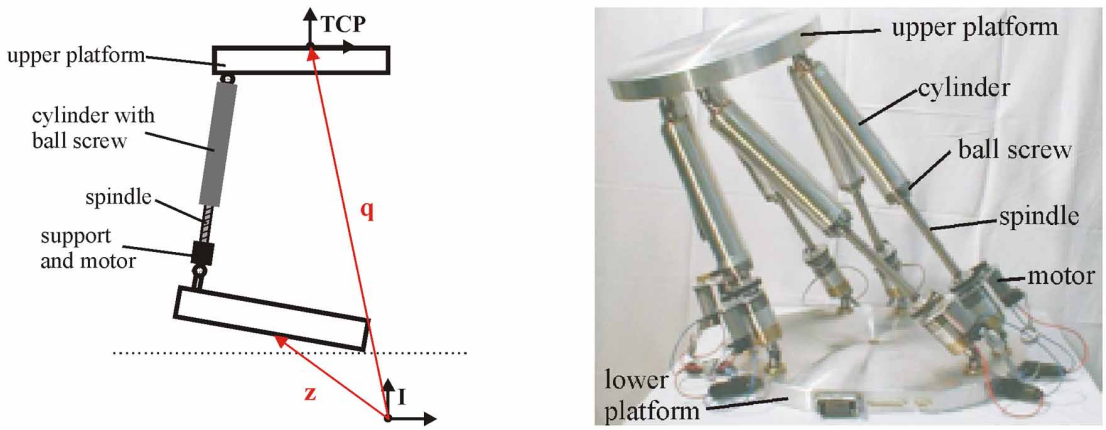

Figure 3: Hexapod topology with one leg (left) and the first version of the test rig (right)

When it is assumed again that the upper platform is in a fixed condition (**q** = constant) and the mechanical vibrations **z** affect the lower platform, then the servo moments M_i which guarantee perfect stabilization of the upper platform can be obtained by

$$\begin{pmatrix} M_1 \\ \vdots \\ M_6 \end{pmatrix} = \mathbf{J}(\mathbf{q},\mathbf{z})^{-T} \left[\mathbf{M}(\mathbf{q},\mathbf{z})\ddot{\mathbf{z}} + \mathbf{G}(\mathbf{z},\dot{\mathbf{z}},\mathbf{q}) + \mathbf{g}(\mathbf{q},\mathbf{z})\right]. \quad (2)$$

Here, **J** is a Jacobi-matrix that projects all forces acting on the TCP in direction of the legs, **M** is the mass matrix, **G** is the matrix of centrifugal and gyroscopic forces and **g** is the matrix which comprises gravitational forces.

6 Stabilization and Tracking Control

The case of *ideal* vibration isolation is finally a force control that is sensitive to parameter uncertainties, external disturbance forces and measurement noise. Thus, undesired TCP motions may occur, because no information about the TCP-states are processed in the control loops. For that reason an additional feedback controller is needed that can compensate possible residual vibrations of the TCP. Further on, the tracking control of the TCP is the second task that the feedback controller should realize. From this follows that each electromechanical axis has now two actuation tasks - the motion tracking and the platform stabilization. Both tasks can be combined if feedback-linearization or computed torque method is applied. Feedback-linearization is a model-based control scheme that has shown to be a very effective for robots that require tracking capabilities [10].
The equations of motion when the TCP is moving and *no vibrations* (**z**=**0**) are present are

$$\mathbf{J}(\mathbf{q})^T \mathbf{F}_{servo} = \mathbf{M}(\mathbf{q})\ddot{\mathbf{q}} + \mathbf{G}(\dot{\mathbf{q}},\mathbf{q}) + \mathbf{g}(\mathbf{q}) \quad (3)$$

where $\mathbf{F}_{servo}$ is the vector containing the six servo forces. The hexapod dynamics are decoupled when the control forces $\mathbf{F}_{servo}$ are chosen as

$$\mathbf{F}_{servo} = \mathbf{J}(\mathbf{q})^{-T} \left(\mathbf{M}(\mathbf{q})\ddot{\mathbf{v}} + \mathbf{G}(\dot{\mathbf{q}},\mathbf{q}) + \mathbf{g}(\mathbf{q})\right) \quad (4)$$

with the new control variable **v**. The dynamics of the hexapod system are now linear and result in six independent double integrators with

$$\ddot{\mathbf{q}} = \ddot{\mathbf{v}}. \quad (5)$$

The double integrators are stabilized with a PD law and the control parameters K_P and K_D are designed by pole placement with the constraint that asymptotic behavior is provided, i.e. no position overshoot occurs. The complete control law that decouples the hexapod and provides perfect tracking is

$$\mathbf{F}_{servo} = \mathbf{J}(\mathbf{q})^{-T} \left(\mathbf{M}(\mathbf{q})\left(diag\{K_P\}\tilde{\mathbf{q}} + diag\{K_D\}\dot{\tilde{\mathbf{q}}}\right) + +\mathbf{G}(\dot{\mathbf{q}},\mathbf{q}) + \mathbf{g}(\mathbf{q})\right), \quad (6)$$

with the control deviation $\tilde{\mathbf{q}}$.
However, if the additional stabilization task is required, then this control law has to be expanded with the feedforward terms of equation (2), which takes into account the undesired vibrations **z**. The resulting control law for stabilization and tracking control needs full state feedback and is obtained by

$$\mathbf{F}_{servo} = \mathbf{J}(\mathbf{q},\mathbf{z})^{-T} \left(\mathbf{M}(\mathbf{q},\mathbf{z})\left(diag\{K_P\}\tilde{\mathbf{q}} + diag\{K_D\}\dot{\tilde{\mathbf{q}}} + \ddot{\mathbf{z}}\right) + \mathbf{G}(\dot{\mathbf{q}},\dot{\mathbf{z}},\mathbf{q},\mathbf{z}) + \mathbf{g}(\mathbf{q},\mathbf{z})\right) \quad (7)$$

Fig. 4 shows the block diagram of the tracking and vibration controller.

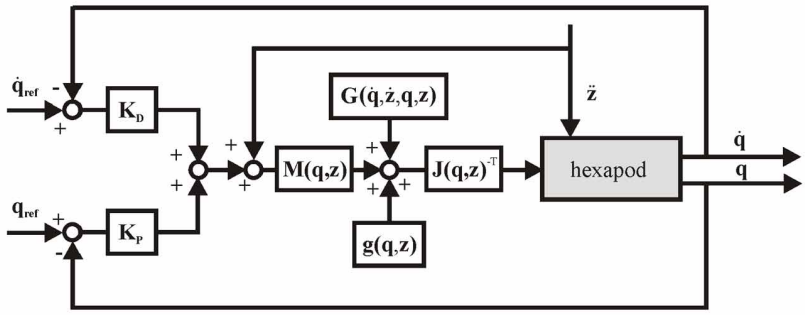

Figure 4: Block diagramm of the coupled stabilization/tracking controller

The task of pure stabilization can be treated as a special case of equation (7). In contrast to the ideal stabilization (equation (2)), the advanced controller measures the TCP-states and uses them in an additional feedforward-feedback loop that is similar to a state controller. Thus, the effect of small imperfections of the hexapod model are reduced and possible residual TCP-vibrations can be compensated.

7 Simulation

Some simulations of the controlled hexapod system have been carried out to quantify the performance of the nonlinear control scheme. The actuators are assumed as ideal torque generators. This first assumption is valid in the desired frequency range ($\leq$ 5 Hz) when the drives have fast inner PID-current controllers. With respect to the realization of the experimental set up, it is necessary to reduce the hexapod model that is used in the control law (equation (7)) to achieve real-time capabilities. Simulations have shown that some effects generated by the equations of motion are small and can be neglected, like the coriolis-forces generated by the cylinders. The resulting real-time control law was programmed in C, implemented as S-function in Matlab/Simulink and coupled with a second model which emulates the test rig that should be controlled. The equations of motion of this second model are represented by differential algebraic equations (DAE) that are derived with the MBS-package Simpack. The communication of both models is provided by Simat, a special Matlab/Simulink interface that establishes a co-simulation between Matlab / Simulink and Simpack.

In the first simulation, the desired TCP condition is $\mathbf{q} = \begin{bmatrix} 0 & 0 & \hat{z} & 0 & 0 & 0 \end{bmatrix}^T$, i.e. the upper platform should be in an inertial fixed position and is just displaced in the vertical direction. The lower platform is excited with noise between 0 Hz and 5 Hz around the two horizontal axis (α, β). The results are shown in Fig. 5.

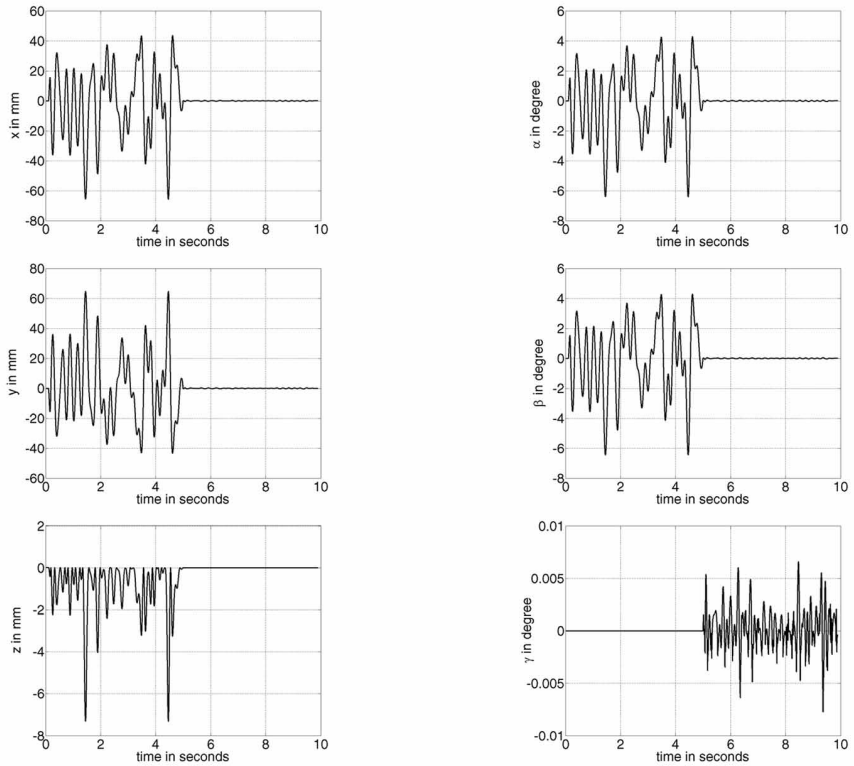

Figure 5: TCP alignment without (<5s) and with (>5s) vibration control (no tracking)

Before t = 5 s, the legs are clamped and no relative velocity between the upper and the lower platform is possible. If the controller is active (t > 5 s), the upper platform is stabilized with a high isolation performance between 42 dB and 59 dB. The coupling of the hexapod-system is reflected in the lower right plot, where the vibrations around the vertical axis (γ) are excited by the controller. But the amplitudes of the induced vibrations are relatively small in comparison with the achieved reduction of the other TCP-coordinates.

The second simulation shows the platform stabilization with an additional tracking task of the TCP. The vibration conditions are the same as in the simulation above and the TCP should track the desired circle-path $\mathbf{q} = \left[\hat{r}\sin(\omega t) \quad \hat{r}\cos(\omega t) \quad \hat{z} \quad 0 \quad 0 \quad 0\right]^T$ in the x-y-plane.

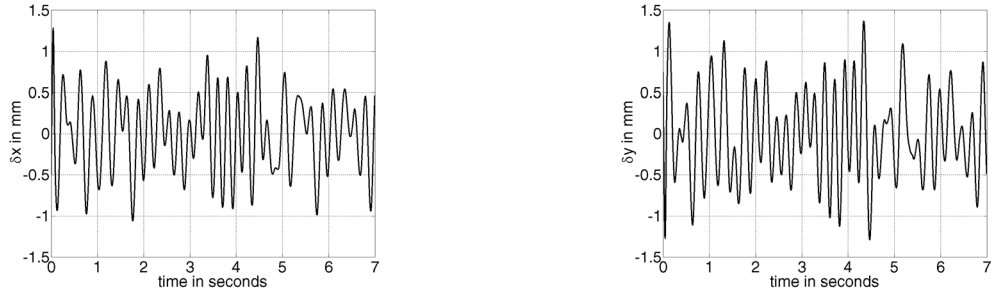

Figure 6: Deviation from the circle in x-y-direction (r_{circle} = 120 mm) during ground vibrations

Fig. 6 shows the corresponding deviations from the reference path of the TCP in the x-y-plane. Again, the applied control strategy of vibration and trajectory control shows its high performance. The maximum path deviation in the x-y-plane when vibrations affect the lower platform is 1.4 mm. The maximum deviation of rotation is 0.18 ° and the deviation in vertical direction is just 0.2 mm. This variations are also very small with respect to the radius of the circle path (120 mm) and the dimension of the excitation (up to 42 mm at the border of the lower platform).

8 Conclusion

The presented nonlinear feedforward-feedback controller has shown its high degree of performance for the combined stabilization and tracking of a hexapod system. Some simulations have demonstrated that the hexapod system can be isolated from undesired ground vibrations. A vibration reduction between 42 dB and 59 dB can be achieved when vibrations (DC-5 Hz) excited the lower platform around the horizontal axes. Additionally, when the hexapod is in tracking mode and the same excitations are present, the root mean square of the TCP-deviation is less than 0.5 mm_{rms} for linear movements and less than 0.05°$_{\text{rms}}$ for angular movements.

To verify the achieved simulation results, the design of a test rig is already in process and will be finished in the near future. The experimental realization will be a challenging task due to some practical requirements, like the limited signal quality of inertial measurement units (IMU) to provide full state feedback.

9 References

[1] Stewart, D.: *A Platform with Six Degrees of Freedom*, Proceedings of the Institution of Mechanical Engineers, Vol. 180, Part I, No. 15, 1965/66.

[2] Gough, V.E.: *Contributions to Discussion to Papers on Research in Automobile Stability and Control in Tyre Performance*, Proc. Auto. Div. Inst. Mech. Engineers, No. 171, pp. 392-394, 1956/57.

[3] Ulbrich, H., Bormann, J., Stenvers, K.-H., Mutzberg, U.: *Active Decoupling of Dynamic Structure-Foundation Interactions*, IUTAM Symposium on Interactions between Dynamics and Control in Advanced Mechnical Systems, Kluwer Academic Publishers, pp. 407-416, 1996.

[4] Anderson, E. H., Leo, D. J., Holcomb, M. D.: *Ultra Quiet Platform for Active Vibration Isolation*, Proceedings of the Society of Photo-Optical Instrumentation Engineers (SPIE), Vol. 2717, pp. 436-451, 1996.

[5] Geng, Z., Haynes, L. S.: *Six-Degree-of-Freedom Active Vibration Isolation Using a Stewart Platform Mechanism*, Journal of Robotic Systems 10(5), pp. 725-744, 1993.

[6] Thayers, D., Vagners, J., Von Flotow, A., Hardham, C., Scribner, K.: *Six-Axis Vibration Isolation System Using Soft Actuators and Multiple Sensors*, Proceedings of the 21st Annual ASS Guidance and Control Conference, 1998.

[7] Honegger, M.: *Nonlinear Adaptive Control of a 6 DOF Parallel Manipulator*, Proceedings of the 4th International Conference on Motion and Vibration Control (MOVIC), Vol. 3, pp. 961-966, Zurich, 1998.

[8] Lebret, G., Liu, K., Lewis, F. L.*: Dynamic Analysis and Control of a Stewart Manipulator*, Journal of Robotic Systems 10(5), pp. 629-655, 1993.

[9] Seunghoon, C., Chanwoo, C., Hyunseok, Y., Yonje, C., Sangjo, L.: *Adaptive Control of a 6 DOF Stewart Platform Based Machine Tool*, Proceedings of the 4th International Conference on Motion and Vibration Control (MOVIC), Vol. 2, pp. 461-466, Zurich, 1998.

[10] Slotine, Li: *Applied Nonlinear Control*, Prentice-Hall, New Jersey, 1991.

[11] Bremer, H.: *Dynamik und Regelung mechanischer Systeme*, Teubner Verlag, Stuttgart, 1998

[12] Gosselin, C. & Angeles, J.: *Singularity Analysis of Closed-Loop Kinematic Chains*, IEEE Transactions on Robotics and Automation, 6(3), pp. 281-290, 1990

[13] Merlet, J.-P.: *Prallel Robots, Solid Mechanics and its Applications*, 74, Kluwer Academic Publisher, Dordrecht / Boston / London, 2000

[14] Ulbrich, H.: *Maschinendynamik*, Teubner Verlag, Stuttgart, 1996